Metabolism Clinical and Experimental 99 (2019) 32–44

Contents lists available at ScienceDirect

Metabolism Clinical and Experimental

journal homepage: www.metabolismjournal.com

Basic Science

Activation of G0/G1 switch gene 2 by endoplasmic reticulum stress enhances hepatic steatosis

Yunqin Ma [a,1], Mingliang Zhang [a,1], Haoyong Yu [a], Junxi Lu [a], Kenneth K.Y. Cheng [b], Jian Zhou [a], Haibing Chen [a,*], Weiping Jia [a,*]

[a] Department of Endocrinology and Metabolism, Shanghai Key Laboratory of Diabetes Mellitus, Shanghai Clinical Center of Diabetes, Shanghai Jiao Tong University Affiliated Sixth People's Hospital, Shanghai, 200233, China
[b] Department of Health Technology and Informatics, The Hong Kong Polytechnic University, Hong Kong 999077, China

ARTICLE INFO

Article history:
Received 18 April 2019
Accepted 28 June 2019

Keywords:
G0/G1 switch gene 2
ER stress
Activating transcription factor 4
Nonalcoholic fatty liver disease

ABSTRACT

Background: Perturbed endoplasmic reticulum (ER) homeostasis and increased levels of G0/G1 Switch Gene 2 (G0S2) have been documented in animal models with fatty liver disease. In this study, we investigated whether G0S2 is regulated by branch of the unfolded protein response (UPR) and contributes to ER stress-induced hepatic steatosis.
Methods: We first analyzed G0S2 expression and the state of the three canonical UPR branches in several hepatic steatosis models, tunicamycin-treated C57BL/6J mice and HepG2 cells, where ER homeostasis was perturbed. We pretreated HepG2 cells with tauroursodeoxycholic acid (TUDCA) to validate whether G0S2 was the downstream target of ER stress. Loss or gain function analysis was conducted to identify which UPR branch specifically linked to G0S2 transcription. The transcription mechanism was estimated by luciferase reporter assay and ChIP assay.
Results: Here we showed that the activation of ER stress was accompanied by elevation of G0S2 expression in the occurrence of fatty liver disease. Furthermore, G0S2 was found to be a novel target gene of activating transcription factor 4(ATF4). We also localized one conserved ATF4-binding sequence in the 5′ regulatory region of *G0S2*, which was responsible for transcriptional activating *G0S2* by ATF4.
Conclusion: G0S2 is regulated by the PERK-eIF2α-ATF4 branch of the UPR and mediates ER stress-induced hepatic steatosis.

1. Introduction

Nonalcoholic fatty liver disease (NAFLD), as the hepatic manifestation of metabolic syndrome, is the most common chronic liver disease and parallels the frequency of central obesity, insulin resistance, metabolic syndrome and type 2 diabetes [1]. An imbalance between lipogenesis and lipid oxidation contributes to the pathogenesis of NAFLD, which is characterized by increased intracellular accumulation of triglycerides in hepatocytes (steatosis) [2]. Although NAFLD is strongly associated with obesity and insulin resistance, its underlying pathogenic mechanisms remains to be further illustrated and therapeutic options are limited.

Recent evidence suggests that endoplasmic reticulum (ER) stress plays a key role in the development of hepatic steatosis [3]. In eukaryotes, ER is the major site of protein folding and maturation as well as lipid metabolism. However, ER homeostasis can be disrupted by inflammation and hyperlipidemia under obese condition. Consequently, the adaptive signaling pathway unfolded protein response (UPR) is triggered to compensate for the ER dysregulation. Chronic activation of UPR is detrimental, which causes inflammation, accelerates progression of NALFD and promotes liver tumor development. The UPR is characterized by the activation of three distinct signal transduction pathways: the PERK-eIF2α-ATF4 pathway, the IRE1α-XBP1 pathway and the

Abbreviations: ATF4, activating transcription factor 4; ATF6, activating transcription factor 6; ATGL, adipose triglyceride lipase; BIP, binding immunoglobulin protein; CHOP, C/EBP homologous protein; CGI-58, comparative gene identification-58; ChIP, chromatin immunoprecipitation; DMSO, dimethyl sulfoxide; ER, endoplasmic reticulum; ERDJ4, ER-localized DnaJ 4; FAS, fatty acid synthase; G0S2, G0/G1 Switch Gene 2; HFD, high fat diet; IRE1α, inositol-requiring enzyme 1α; Luc, luciferase; MCD, methionine and choline-deficient; NAFLD, nonalcoholic fatty liver disease; NASH, non-alcoholic steatohepatitis; PA, palmitic acid; PERK, PKR-like endoplasmic reticulum kinase; SCD1, stearoyl-CoA desaturase-1; SREBP, Sterol regulatory element binding protein; TG, triglyceride; Tm, tunicamycin; TUDCA, tauroursodeoxycholic acid; UPR, unfolded protein response; XBP1, X-box binding protein 1.

* Corresponding authors at: Shanghai Key Laboratory of Diabetes Mellitus, Dept. of Endocrinology and Metabolism, Shanghai Jiao Tong University Affiliated Sixth People's Hospital, 600 Yishan Rd., Shanghai, 200233, China.
E-mail address: wpjia@sjtu.edu.cn (W. Jia).

[1] The two authors contributed equally to this work.

https://doi.org/10.1016/j.metabol.2019.06.015
0026-0495/

activating transcription factor 6(ATF6) pathway [4]. X-box binding protein 1 (XBP1) and activating transcription factor 4 (ATF4) are downstream of inositol-requiring enzyme 1α (IRE1α) and PKR-like endoplasmic reticulum kinase (PERK). XBP1 and ATF4 have been reported to regulate hepatic lipogenesis by directly binding to the promoters of a subset of lipogenic genes and activating their expression, such as fatty acid synthase (FAS), and stearoyl-CoA desaturase-1 (SCD1) [4–7]. Nuclear ATF6 interacts and antagonizes sterol regulatory element binding protein-2 (SREBP2) to restrain the transcription of lipogenic genes and lipid accumulation [8]. Although there is evidence to support that all three UPR pathways could induce steatosis by stimulating lipogenesis, it remains uncertain whether a stressed UPR plays a role in regulating hepatic lipolysis. This is an important issue to be addressed.

Lipolysis is mainly controlled by adipose triglyceride lipase (ATGL), which is regulated by comparative gene identification-58 (CGI-58) and G0/G1 switch gene 2 (G0S2). G0S2 inhibits and CGI-58 activates ATGL activity [9]. G0S2, which is highly expressed in the liver, is originally found to be expressed in cultured mononuclear cells during the drug-induced cell cycle transition from G0 to G1 phase [10]. G0S2 is required for rapid metabolic adaptations as its level changes according to the nutritional status. G0S2 level in the liver is elevated in response to fasting, which favors hepatic fat deposition and reduces fatty acid oxidation. The reverse is true during re-feeding [11]. The relationship between G0S2 expression and hepatic steatosis has been established in liver-specific genetic mouse models with deletions or over expression of G0S2. G0S2 knockout mice displayed a drastic decrease in hepatic triglyceride (TG) content and were resistant to HFD-induced liver steatosis [11,12]. Overexpression of G0S2 induced TG accumulation in the mouse liver by reducing lipolysis rate to accelerate the development of hepatic steatosis [13]. Considering the important role of G0S2 as a regulator of TG content in the liver, down-regulation of G0S2 could represent one potential therapeutic strategy for the treatment of hepatic steatosis.

Base on the concept of G0S2 as a "master regulator" of lipolytic rates and the role of ER stress in lipid metabolism [14], we sought to answer the following questions: 1) How the disrupted ER homeostasis contributes to the development of NAFLD? 2) Whether G0S2 is a UPR mediator linked to the progression of NAFLD? Here, we used various ER stress mouse models and cell systems to study the interplay between ER stress and G0S2 during the development of hepatic steatosis. In addition, we conducted loss-of-function analysis to prove which branch of UPR is responsible for G0S2 regulation.

2. Materials and methods

2.1. Animal experiments

Male C57BL/6J mice were purchased from Shanghai Laboratory Animal Center, CAS (SLACCAS). Male leptin-deficient *ob*/*ob* mice (*ob*/*ob*) with C57BL/6J genetic background were generously provided by Dr. Jia Li of the Shanghai Institute of Materia-Medica, Chinese Academy of Sciences. Mice were housed in laboratory cages under controlled temperature(23 ± 3 °C) and humidity conditions (35 ± 5%) in an artificial 12-hour light/dark cycle (7:00–19:00) with free access to water and food. For the diet-induced obesity model, 8-week-old C57BL/6J mice were fed a standard diet containing 10% kcal of fat (Chow diet, Shanghai Laboratory Animal Co. Ltd) or a high fat diet containing 60% kcal of fat (HFD) (Catalog number D12492, Research Diets Inc.) for 16 weeks. For the diet-induced non-alcoholic steatohepatitis (NASH) model, 8-week-old C57BL/6J mice were fed methionine and choline-deficient diet (MCD) (Catalog numberA02082002B, Research Diets Inc.) or MCD control diets (Chow diet) (Catalog numberA02082003B, Research Diets Inc.) for 8 weeks. For the tunicamycin-induced ER stress model, male C57BL/6J mice at 10th week were randomly assigned to different groups and administered with Dimethyl Sulfoxide (DMSO) or tunicamycin (1 mg/kg body weight, Sigma) intraperitoneally. Mice were sacrificed after the indicated times (2 h, 4 h, 8 h and 12 h) under anesthetic conditions. Livers, hearts, skeletal muscles were harvested and snap-frozen in liquid nitrogen and subsequently stored at −80 °C. All animal experimental protocols were approved by the Animal Care Committee of Shanghai Jiao Tong University Affiliated Six People's Hospital in accordance with the Guidelines for the Care and Use of Laboratory Animals.

2.2. Human liver samples

Human liver tissue samples were collected from patients of benign focal hepatic lesions undergoing liver surgery at the Department of Liver Surgery (Zhongshan Hospital, Fudan University, Shanghai, China), including tissues from patients with NAFLD as described previously [15]. Diagnosis of NAFLD was according to the guidelines proposed by the Asia-Pacific Working Party [16]. Tissues were immediately snap frozen in liquid nitrogen and stored at −80 °C. Five patients with NAFLD whose hepatic steatosis scored as grade 1 to 2 and NAFLD activity score (NAS) was graded as 1 to 4 were enrolled in this study. Five samples with 0 degree of steatosis were referred to as normal control in this study whose NAFLD activity score (NAS) graded 0 to 1 [17]. Relevant donor information was listed in Supplemental Table 2. Local ethics committee approved the study procedures as it followed the principles of the Declaration of Helsinki. Before their participation all subjects provided written informed consents.

2.3. Cell culture and treatment

Human hepatoma cell line HepG2, HEK-293T cells used in this study was from American Type Culture Collection (ATCC). IRE1$^{-/-}$ MEF cells and their wild-type counterparts were the generous gifts from Dr. Yong Liu (Wuhan University). All of them were grown in DMEM supplemented with 10% fetal bovine serum, 2 mM glutamine, 100 units/ml penicillin and 100 mg/ml streptomycin (Pierce Thermo Fisher Scientific). For ER stress experiments, HepG2 cells were incubated in DMEM containing DMSO or tunicamycin (10 μg/ml, Sigma) for indicated times prior to protein extraction or total RNA isolation. HepG2 cells were treated with 5 mM TUDCA (Sigma) to suppress ER stress signaling 0.5 h prior to and during tunicamycin (10 μg/ml) treatment.

2.4. Isolation of primary hepatocytes and treatment

Primary hepatocytes were isolated from male mice at 8–10 weeks of age. Briefly, washing buffer (Calcium-free Kreb-Ringer buffer containing 0.1% glucose and 1 mM EGTA) was perfused through the portal vein to flush out the blood before switching to perfusion buffer (Kreb-Ringer Buffer containing 0.1% glucose and 5 mM $CaCl_2$) with collagenase. When perfusion is completed, carefully excise the liver and filter the cells through a 70 μm cell strainer (BD Falcon). Wash cells with cold perfusion buffer three times and resuspend cells in cold HepatoZYME-SFM medium (Invitrogen) supplemented with 2 mM glutamine, 20 units/ml penicillin, and 20 μg/ml streptomycin. Cells were plated at 2×10^5 cells/well in 12-well dishes. Eight hours later, primary mouse hepatocytes were incubated with 10 μg/ml tunicamycin for 2 h, 6 h and 10 h or exposed to TUDCA 0.5 h prior to and during tunicamycin treatment.

2.5. Lipid extraction and measurement

To determine hepatic/cardiac/skeletal muscle TG level, tissues were homogenized in phosphate-buffered saline (PBS), followed by mixing sufficiently with CHCl3/CH3OH (2:1, volume/volume). The lower organic phase after centrifugation was dried with nitrogen. The organic phase was dissolved in absolute ethanol with 1% Triton X-100 for TG

measurement using a commercial triglyceride determination kit (Bioassay Systems).

2.6. Quantitative real-time PCR analysis

Total RNAs were isolated from cells or liver tissues by TRIzol reagent (Pierce Thermo Fisher Scientific) and were reverse transcribed into cDNA using a High-Capacity cDNA Reverse Transcription Kit (Pierce Thermo Fisher Scientific). Quantitative real-time PCR was conducted with an ABI Prism 7500 sequence detection system, using the SYBR Green PCR Master Mix (Applied Biosystems). *18s* rRNA was used as an internal control for normalization. Primer pairs used were listed in Supplementary Table 1, which were designed using Primer Express software (Applied Bio-systems) based on GenBank sequence data. The experiments themselves were repeated 3 times independently. Each sample testing was repeated twice in each independently experiment. The sequences of primer pairs (forward and reverse) were same in three independent experiments.

2.7. Western blot analysis

For immunoblotting analysis, total proteins were extracted using RIPA lysis buffer. The proteins were transferred onto a polyvinylidene difluoride membrane filters after sodium dodecyl sulfate polyacrylamide gel electrophoresis (SDS-PAGE). The blocked membranes were incubated with primary antibodies overnight at 4 °C and secondary antibodies for 2 h at room temperature. Proteins were visualized with ECL Western blotting detection reagents (Pierce Thermo Fisher Scientific). The following antibodies were used in this study: BIP (Cell Signaling Technology, Inc.CAT #3177), p-IRE1α(Ser724) (Novus Biologicals, Inc. CAT #NB 100-2323), t-IRE1α (Cell Signaling Technology, Inc. CAT #3294), p-eIF2α (Ser51) (Cell Signaling Technology, Inc. CAT #9721), t-eIF2α (Cell Signaling Technology, Inc. CAT #9722), ATF4 (Cell Signaling Technology, Inc. CAT #11815), ATF6 (Cell Signaling Technology, Inc. CAT #65880), XBP1 (Abcam, CAT ab37152), G0S2 (Santa Cruz Biotechnology, Inc. CAT Sc-518067), β-tubulin (Sigma, CAT 05-661).

2.8. Transient transfection with small interfering RNA (siRNA)

siRNAs against human genes including *ATF4*, *ATF6* and *XBP1* were synthesized by Gene Pharma Co. Ltd. (Shanghai, China). *ATF4* siRNA: 5′-CUGCUUACGUUGCCAUGAUTT-3′, *ATF6* siRNA: 5′-GGGCTCATAC AGATGCCACTA-3′. *XBP1* siRNA: 5′- UCGGUAUGGAAUUUGUUUC-3′. HepG2 cells were grown to 70–80% confluence and then transfected with siRNAs for *ATF4*, *ATF6*, *XBP1* and scramble siRNA as control respectively using RNAiMAX Transfection Reagent (Pierce Thermo Fisher Scientific) according to the manufacturer's instructions. After 48 h the transfected cells were treated with tunicamycin for 6 h.

2.9. Overexpression of ATF4

The pcDNA3.1-ATF4 plasmid was kindly provided by Dr. Xu Shen from Shanghai Institute of Materia-Medica, Chinese Academy of Sciences. For transient overexpression in HepG2 cells, transfection was performed using Lipofectamine 2000 (Invitrogen) according to the manufacturer's instructions.

2.10. Oil-red O staining

HepG2 cells were transfected with pcDNA3.1-ATF4 plasmid for 6 h and then infected with lentivirus encoding siRNA targeting G0S2 which was synthesized by Gene Pharma Co. Ltd. (Shanghai, China). After 24 h, HepG2 cells were exposed to palmitic acid (PA) (Sigma) for 12 h. Subsequently, cells were fixed in formalin and incubated in Oil-red O solution for 10 min before hematoxylin staining. Each sample was analyzed by inverted microscope. Oil-red O dye was eluted by isopropyl alcohol and the absorbance was measured at 520 nm.

2.11. Luciferase reporter assays

The 3000 bp promoter sequence in upstream regulatory region of G0S2 was amplified from HepG2 cells genomic DNA using the forward primer 5′-CGGGGTACCTCAAAAAAAGGAACTGAGCTGGTGATGTG-3′ and reverse primer 5′-GGAAGATCTCTTCCTCCCTAGTGCAAAATGGTA GACGC-3′. After excising with *Kpn*I and *Bgl*II, the amplified fragment was cloned into pGL3-basic vector to form the luciferase reporter plasmids of the human *G0S2* promoter. For luciferase activity assays, the *G0S2* promoter luciferase reporter plasmid and the pcDNA3.1-ATF4 was co-transfected into 293T cells along with a Renilla-expressing plasmid for normalization. In tunicamycin-induced luciferase activity assay, 293T cells were added fresh culture medium supplemented with tunicamycin (10 μg/ml) after overnight transfection of *G0S2* promoter luciferase reporter plasmids and a Renilla-expressing plasmid. Luciferase activity was measured using Dual-Luciferase™ reporter assay system (Promega) following the manufacturer's Instructions, and results were calculated as the relative light units (RLUs) of the firefly luciferase to the Renilla luciferase. Deletion TTGCAT in the wild-type *G0S2* reporter construct was generated with primer: forward primer 5′-CTGCAAAGGCTGTTGCAAGACACTGACCTTTGCAATTTTC-3′ and reverse primer 5′-TCAAGTATGGAAGGGGCTGTTGGTAGAAGT-3′. *G0S2* promoter deletion mutation was confirmed by DNA sequence. Promoter activities of deletion mutation were measured as above.

2.12. Chromatin immunoprecipitation (ChIP)

ChIP assays was carried out in liver from C57BL/6J treated with either DMSO or tunicamycin in accordance with the manufacturer's protocol. DNA-protein crosslinking was performed by incubating powdered liver tissue with 1% formaldehyde in PBS containing 1 mM dithiothreitol and 1 mM phenylmethylsulfonyl fluoride for 15 mins. After incubation chromatin extract overnight with antibody against ATF4 (Cell Signaling) or control IgG (Santa Cruz Biotechnology), DNA was purified and used in quantitative real-time PCR with specific primers. The sequence of the primers used: forward primer 5′-ATGCCTTTA TAGCCCCTCT-3′, and reverse primer 5′-GTCATGAGCAGCAATCCACA-3′ for ATF4-binding element; and forward primer 5′-GGACTGTGG GTTTCTGTGCT-3′ and reverse primer 5′-ATCTCCAGGTGGGCTTCTGT-3′ for the unrelated control.

2.13. Statistical analysis

All statistical analyses were performed with the statistical package for social sciences (SPSS) version 22.0 software or Prism 6 (GraphPad Software). Normality was assessed by a Shapiro-Wilks test and all variables were normally distributed. Levene's test was used to assess the homogeneity of variance and all variables in our study had homogeneous variances. Results were presented as the mean ± SEM. Statistical analysis was assessed using a two-tailed Student's *t*-test to compare values between two groups. The significance of the difference between multiple groups was evaluated using one-way or two-way analysis of variance followed by Bonferroni's post hoc test. * $P < 0.05$ was identified statistically significant; ** $P < 0.01$, very significant; *** $P < 0.001$, extremely significant. $P > 0.05$ was considered not significant (NS). The number of animals used for each experiment was indicated in the figure captions. Data were representative of at least three independent experiments.

3. Results

3.1. G0S2 expression increased along with activated ER stress in liver samples from NAFLD patients

We examined whether ER stress accompanied change of G0S2 level in liver tissue of patients with or without NAFLD. we observed elevated mRNA abundance of ATF4 and C/EBP homologous protein (CHOP) (Fig. 1A and B) and higher expression levels of the UPR markers in liver samples of NAFLD patients, including p-IRE1α, p-eIF2α, ATF6 and ATF4 (Fig. 1D). We also detected increased G0S2 in liver from patients with NAFLD (Fig. 1C and D). These results demonstrated that the up-regulation of hepatic G0S2 expression and activation of ER stress co-existed in human fatty liver.

3.2. G0S2 expression increased in parallel with activated ER stress in liver tissue from HFD-fed mice

To investigate a putative link between G0S2 and ER stress in hepatic steatosis, we examined the expression of ER stress markers and G0S2 in hepatic steatosis mouse model. Consistent with the development of obesity, HFD-fed mice showed an increase in hepatic TG levels (Fig. 2A) and exhibited much higher body weight (Supplementary Fig. 1A) when compared with chow diet-fed mice (Chow). In parallel with up-regulated mRNA expression of *Atf4* and *Chop* (Fig. 2B and C), the mRNA abundance of *G0s2* was significantly increased in livers of HFD-fed mice (Fig. 2D). The phosphorylation of IRE1α and eIF2α increased significantly along with up-regulation of ATF4 and ATF6, which were accompanied by increased G0S2 protein levels in livers of HFD-fed mice (Fig. 2E). In addition, we also observed elevated abundance of G0S2 in hearts of HFD-fed mice along with up-regulation of ATF4 and increased phosphorylation of IRE1α (Supplementary Fig. 5B). In skeletal muscles of HFD-fed mice, G0S2 protein was also prominently up-regulated, in parallel with significantly increased TG content. However there were no significant differences in the content of various ER stress indicators in skeletal muscles between chow diet-fed and high-fat diet-fed mice (Supplementary Fig. 6B). The results implied that the elevated expression of G0S2 was in parallel with the occurrence of metabolic ER stress in liver and other organs that was sensitive to ER stress such as the heart.

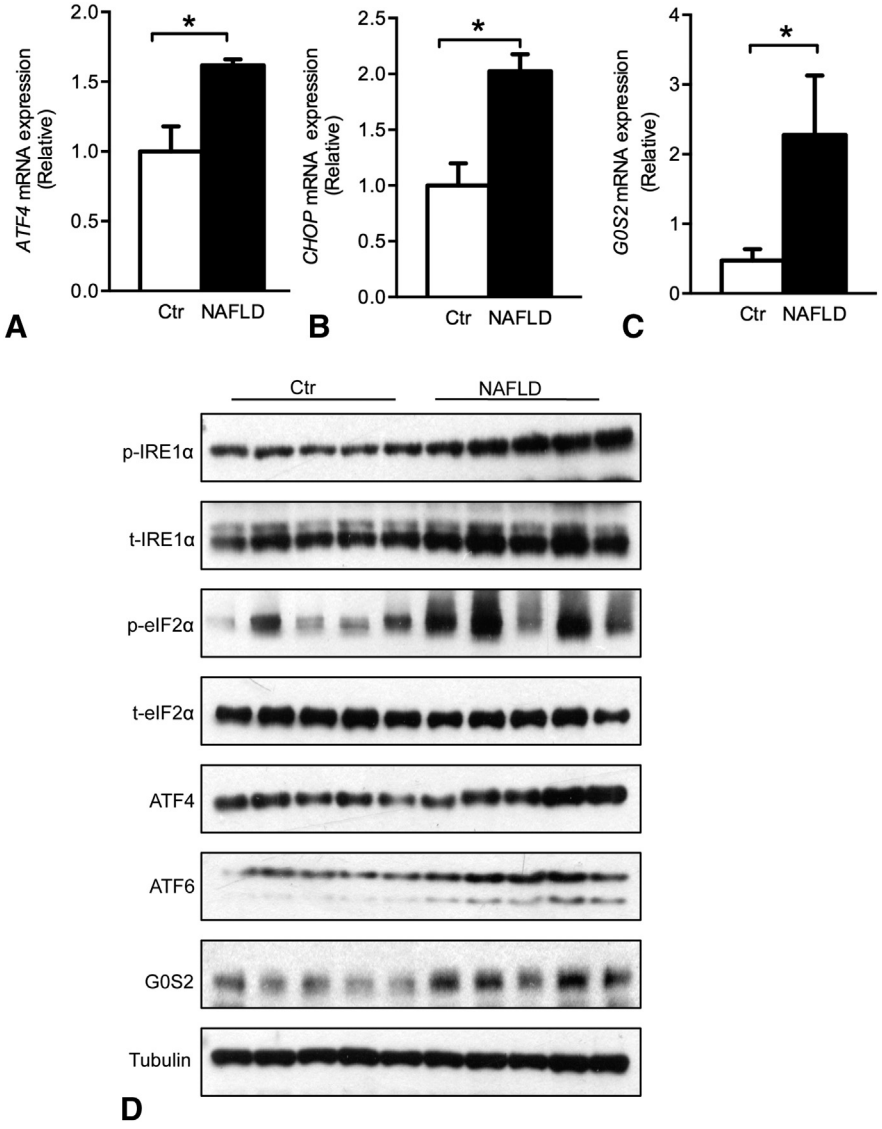

Fig. 1. Hepatic UPR activation and G0S2 expression in NAFLD. Human hepatic tissue samples were prepared from patients with or without NAFLD ($n = 5$/group). (A, B and C) The mRNA abundance of *ATF4, CHOP* and *G0S2* in human fatty liver disease. (D) The phosphorylation of IRE1α and eIF2α and ATF4, ATF6 and G0S2 protein abundance in whole liver lysates were analyzed by immunoblotting. Tubulin was used as the loading control. All the results were shown as the mean ± SEM. Error bars represent the SEM. Statistical significance $^{*}p < 0.05$ of NAFLD group relative to the control group determined by two-tailed Student *t*-test.

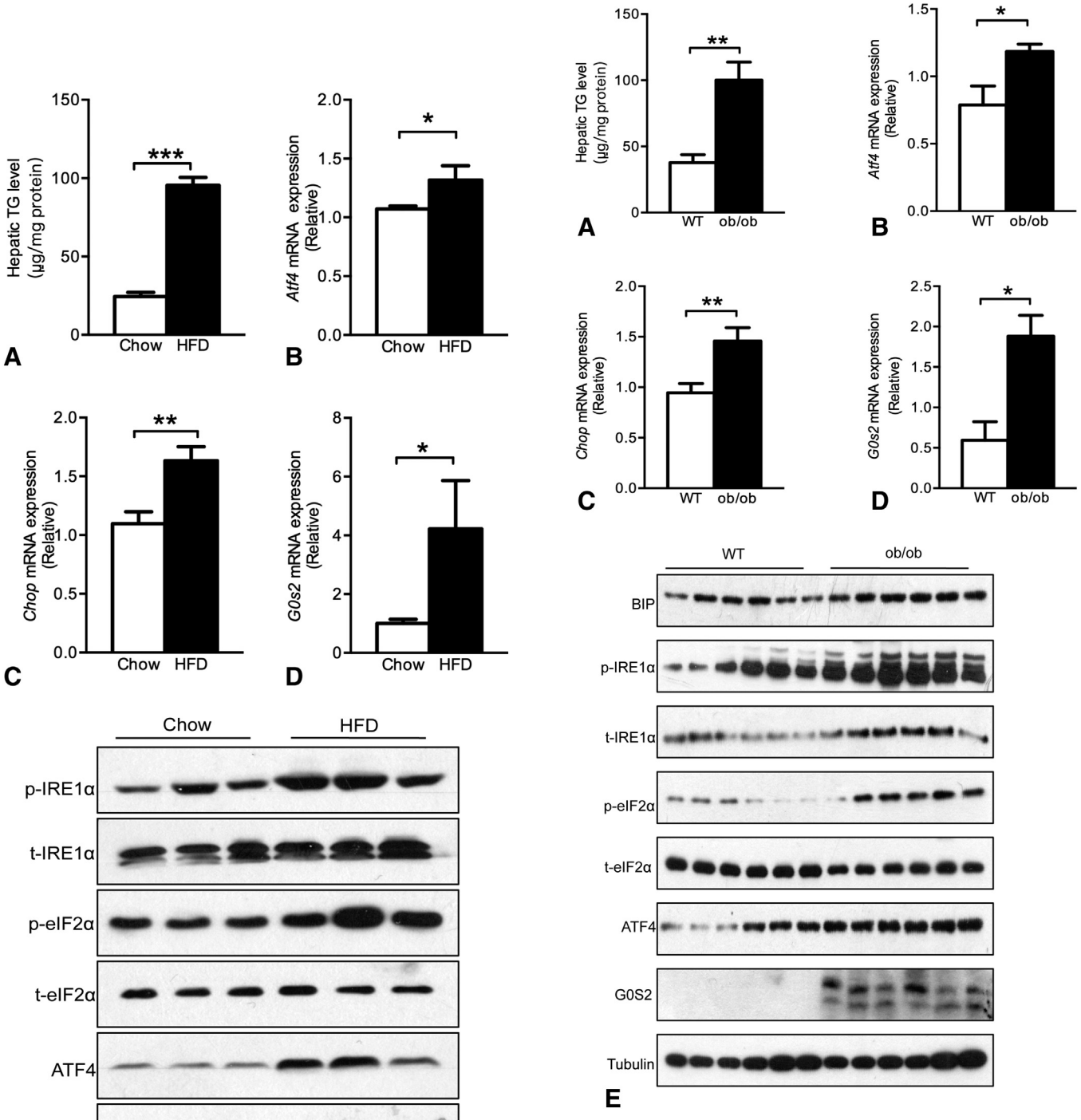

Fig. 3. Hepatic UPR activation and G0S2 expression in *ob*/*ob* mice. Male *ob*/*ob* mice compared to WT mice at three months of age ($n = 6$/group). (A) Hepatic levels of TG. (B, C and D) The mRNA abundance of *Atf4, Chop* and *G0 s2*. (E) Expression of UPR markers: BIP, p-IRE1, p-eIF2α, ATF4 and G0S2 protein were analyzed by immunoblotting in mice liver tissue lysates. Tubulin was taken as the loading control. All the results were shown as the mean ± SEM. Error bars represented the SEM. Statistical significance $^{*}p < 0.05$, $^{**}p < 0.01$ represented *ob*/*ob* subjects relative to the WT subjects and was determined by two-tailed Student *t*-test.

Fig. 2. Effect of HFD on hepatic UPR activation and G0S2 expression. Male C57BL/6 J were fed a low-fat diet (Chow, n = 5) or a high-fat diet (HFD, n = 5) for 16 weeks. (A) Hepatic levels of TG. (B, C and D) The mRNA abundance of *Atf4, Chop* and *G0 s2*. (E) UPR markers p-IRE1α, p-eIF2α, ATF4, ATF6 and G0S2 protein abundance in whole liver lysates were analyzed by immunoblotting. Tubulin was taken as the loading control. All the results are shown as the mean ± SEM. Error bars represent the SEM. Statistical significance $^{*}p < 0.05$, $^{**}p < 0.01$, $^{***}p < 0.001$ represented HFD subjects relative to the Chow subjects and was determined by two-tailed Student *t*-test.

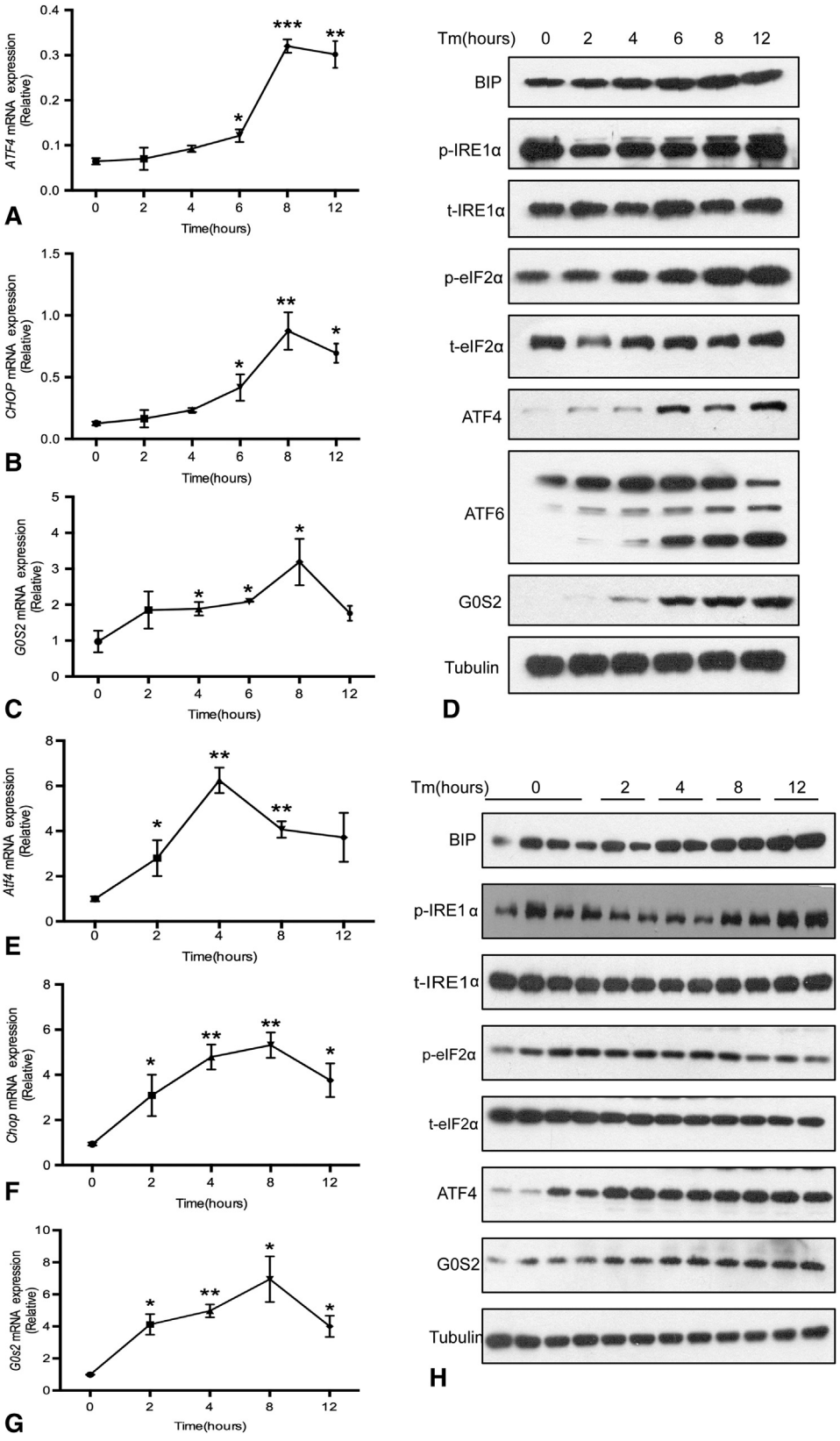

Fig. 4. ATF4 induces the expression of G0S2 in vivo and in vitro. HepG2 cells were treated with tunicamycin (Tm, 10 μg/ml) or DMSO for different times (0, 2 h, 4 h, 6 h, 8 h and 12 h) and DMSO (vehicle) as control. (A, B, and C) Time course of mRNA abundance of *ATF4, CHOP* and *G0S2* in HepG2 cells incubated with Tm at different time points ($n = 3$ for each time point) were determined by quantitative real-time PCR ($n = 3$ for each time point). (D) The protein abundance changes of BIP, ATF4, ATF6, G0S2 and the phosphorylation of IRE1α and eIF2α were analyzed by immunoblotting (n = 3). Male C57BL/6J mice were treated with Tm (1 mg/kg body weight) at different time intervals (0, 2 h, 4 h, 8 h and 12 h) and PBS (vehicle) as control. (E, F and G) *Atf4, Chop* and *G0s2* mRNA abundance in liver tissues after injection of Tm were determined by quantitative real-time PCR ($n = 3$–4 for each time point). (H) The protein abundance of BIP, ATF4, G0S2 and the phosphorylation of IRE1α and eIF2α were analyzed by immunoblotting (n = 3–4). All the results were shown as the mean ± SEM. Error bars represent the SEM. Statistical significance * $p < 0.05$, ** $p < 0.01$, ***$p < 0.001$ represented Tm group at different times compared to initial control group (vehicle), which was determined by one-way ANOVA.

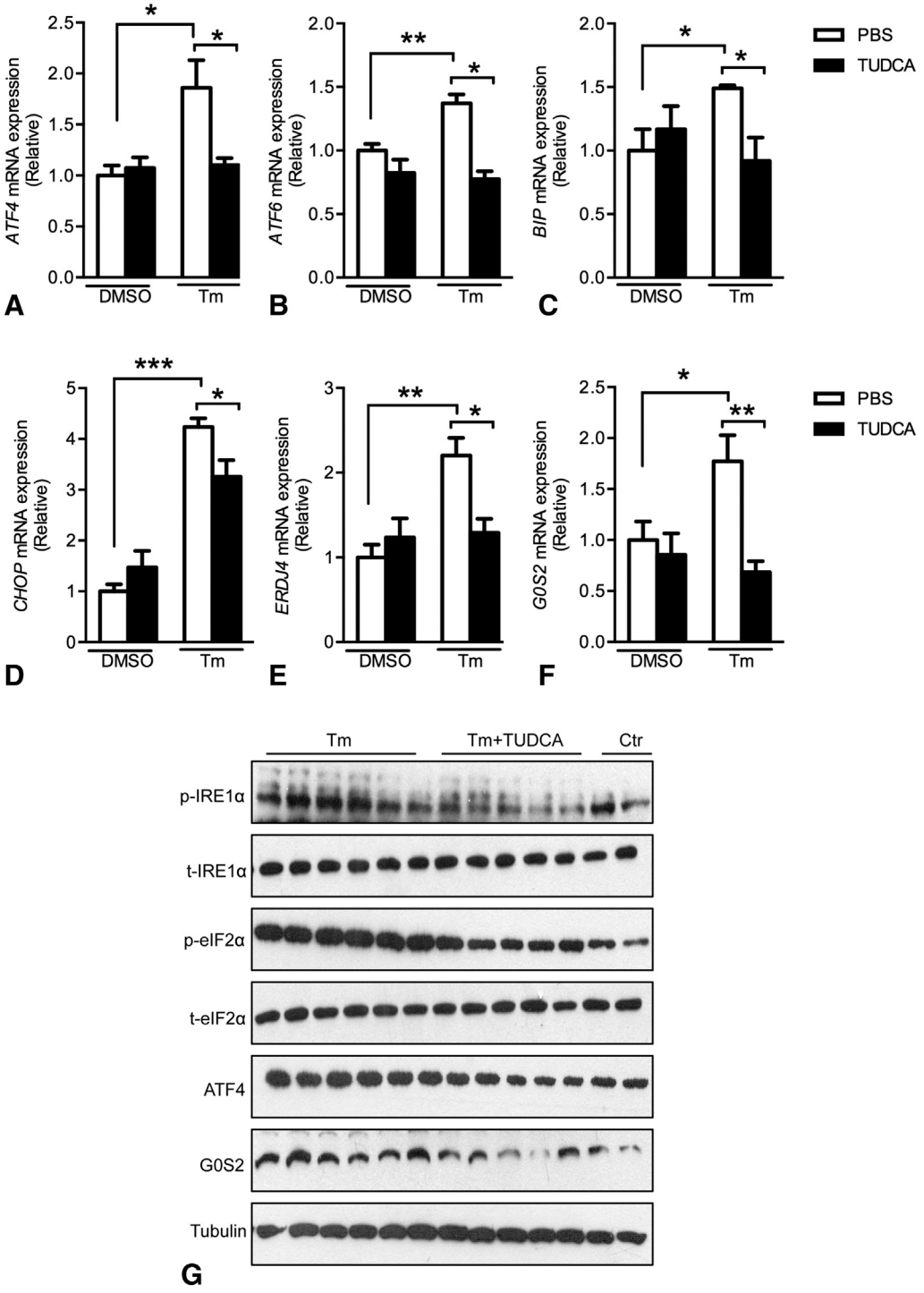

Fig. 5. TUDCA prevents ER stress-induced G0S2 increase in vitro. We exposed HepG2 cells to chemical chaperones TUDCA (5 mM) 0.5 h prior to incubating with Tm (10 μg/ml). (A, B, C, D, E and F) *ATF4, ATF6, BIP, CHOP, ERDJ4* and *G0S2* mRNA abundance were determined by quantitative real-time PCR after co-incubation with Tm and TUDCA in HepG2 cells($n = 3$ for each time point). (G) The protein abundance of ATF4, G0S2 and the phosphorylation of IRE1α and eIF2α in HepG2 cells treated with Tm (10 μg/ml) and/or TUDCA(5 mM). All the results were shown as the mean ± SEM. Error bars represented the SEM. Statistical significance * $p < 0.05$, ** $p < 0.01$, *** $p < 0.001$ was determined by two-way ANOVA.

Fig. 6. PERK-eIF2α-ATF4 Pathway is responsible for the regulation of G0S2. HepG2 cells were transfected with siRNA for *ATF6, ATF4, XBP1* and scramble siRNA (control) respectively. After transfection 48 h, Quantitative real-time PCR and immunoblotting were used to determine the silencing efficiency of siRNAs and related genes changes (n = 3). (A, B, C and D) *ATF4*, *ATF6*, *XBP1* and *G0S2* mRNA was analyzed by quantitative real-time PCR using 18S rRNA quantitation for normalizing. *$p < 0.05$; **$p < 0.01$ determined by one-way ANOVA. (E) Expression of ATF4, ATF6, XBP1 and G0S2 protein were analyzed by immunoblotting in lysates from HepG2 cells. Tubulin was taken as the loading control. $IRE1^{-/-}$ MEF cells (KO) and $IRE1^{+/+}$ MEF cells (WT) were treated with DMSO or Tm (10 μg/ml) for 6 h. (F, G and H) Quantitative real-time PCR was used to analyze *Xbp1, Chop and G0s2* mRNA in MEF cells. HepG2 cells were transfected with ATF6 siRNA or control. After 48 h the transfected cells were then treated with DMSO or Tm (10 μg/ml) for 6 h (n = 3). (I, J and K) Quantitative real-time PCR was used to analyze *ATF6, CHOP* and *G0S2* mRNA. Results were shown as the mean ± SEM. NS, no significance;* $p < 0.05$; ** $p < 0.01$, *** $p < 0.001$ determined by two-way ANOVA.

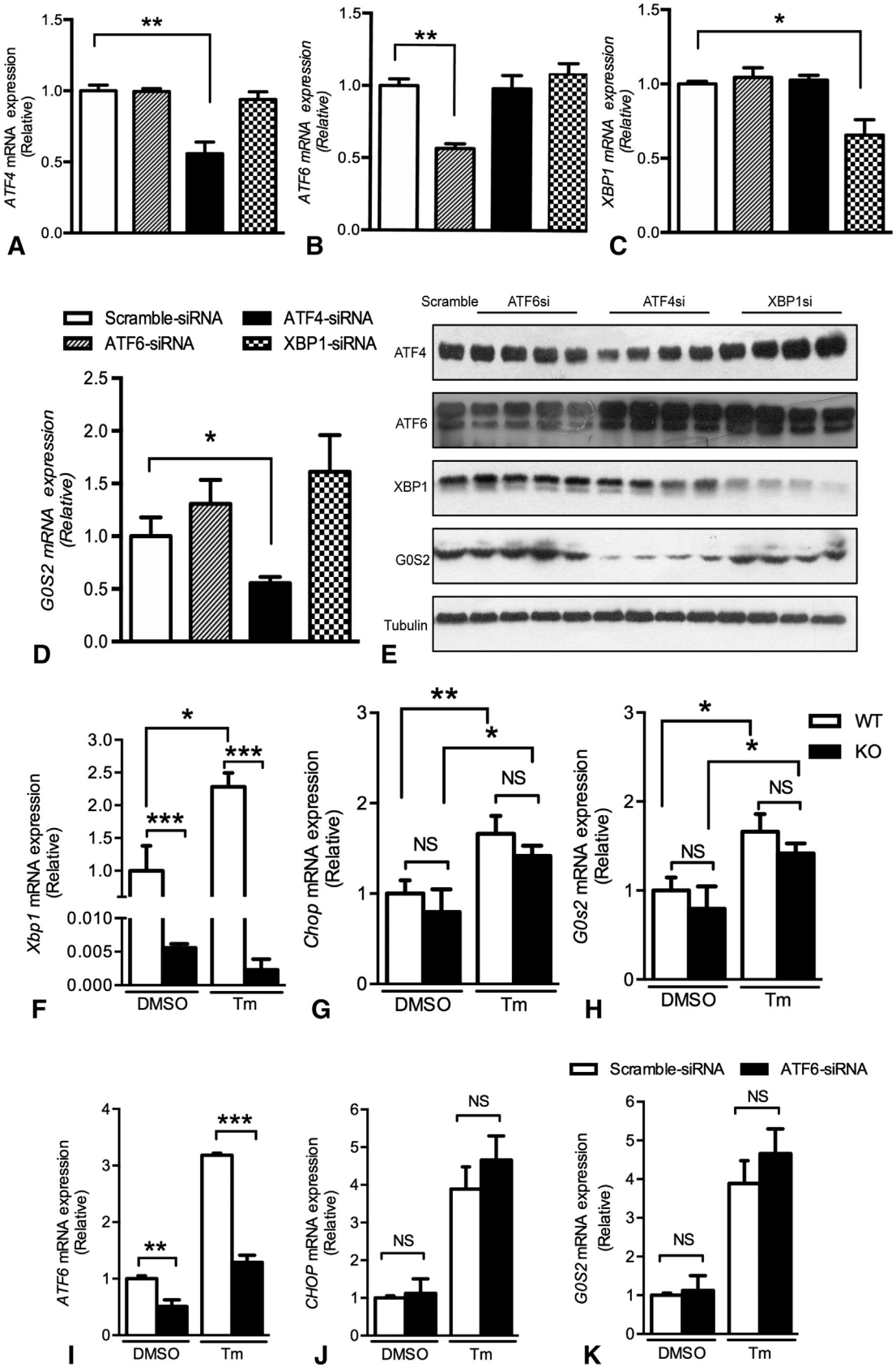
ATF4 mRNA expression (Relative)
ATF6 mRNA expression (Relative)
XBP1 mRNA expression (Relative)
A
B
C
Scramble-siRNA
ATF6-siRNA
ATF4-siRNA
XBP1-siRNA
G0S2 mRNA expression (Relative)
D
Scramble
ATF6si
ATF4si
XBP1si
ATF4
ATF6
XBP1
G0S2
Tubulin
E
Xbp1 mRNA expression (Relative)
F
Chop mRNA expression (Relative)
G
G0s2 mRNA expression (Relative)
H
WT
KO
DMSO
Tm
NS
ATF6 mRNA expression (Relative)
I
CHOP mRNA expression (Relative)
J
G0S2 mRNA expression (Relative)
K

3.3. G0S2 expression was associated with activated ER stress and hepatic steatosis in liver tissue from ob/ob mice

Both the above NAFLD model and the HFD model exhibited a similar trend in the expression of G0S2 and ER stress markers. To further investigate the link between ER stress and G0S2, we employed *ob*/*ob* mice model, a genetic murine steatosis model to verify the relationship between UPR branches and G0S2. Fatty liver was confirmed by hepatic TG test (Fig. 3A). Interestingly, we noted a striking increase in the expression of binding immunoglobulin protein (BIP), ATF4 and the phosphorylation of IRE1α and eIF2α in *ob*/*ob* mice (Fig. 3E). Furthermore, mRNA expression and protein abundance of G0S2 was also increased in *ob*/*ob* mice compared to WT mice (Fig. 3D and E). These results further indicated the link between ER stress and G0S2. Furthermore, we also found a similar link in mice model of NASH (Supplementary Fig. 2).

3.4. Expression of G0S2 was induced under experimental ER stress

To determine whether the increased hepatic G0S2 expression is linked to changes of ER stress, we challenged C57BL/6J mice or HepG2 cells with the chemical ER stress-inducing agent tunicamycin and monitored the changes at different time points. The response of ER stress markers and G0S2 in HepG2 cells increased in parallel, and their maximum levels were reached after 8 h (Fig. 4A–D). In C57BL/6J mice treated with tunicamycin, mRNA abundance of *Atf4, Chop* and *G0s2* reached the peak level after 8 h (Fig. 4E–G). The protein levels of ATF4, ATF6 surged at 6 h and kept at a high level until 12 h. G0S2 protein increased during tunicamycin-induced ER stress in a time-dependent manner (Fig. 4H). In addition, we observed significantly elevated expression of ER stress markers in isolated primary mouse hepatocytes incubated with tunicamycin (Supplementary Fig. 3A–C). Taken together, the above experimental ER stress models both in vitro and in vivo exhibited similar response patterns of G0S2.

3.5. TUDCA prevented ER stress-induced G0S2 in vitro

To further validate if the modulation of G0S2 proteins is a direct effect of ER stress in the liver, we exposed HepG2 cells to chemical chaperones TUDCA to relieve ER stress. TUDCA marginally inhibited the marked activation of *ATF4, ATF6, BIP, CHOP* and *ER-localized DnaJ 4 (ERDJ4)* triggered by tunicamycin (Fig. 5A–E). Importantly, TUDCA also significantly diminished ER stress-induced G0S2 expression (Fig. 5F–G). We also noted a similar change of G0S2 in TUDCA-treated primary mouse hepatocytes (Supplementary Fig. 3D).

3.6. PERK-eIF2α-ATF4 pathway was responsible for the regulation of G0S2

To test whether G0S2 was a common downstream target of multiple UPR pathway(s), loss-of-function analysis was conducted by transfecting HepG2 cells with siRNA against *ATF4, ATF6* and *XBP1*. Immunoblotting analysis revealed that siRNA-mediated knockdown of *ATF4, ATF6* and *XBP1* was successful (Fig. 6A-C). siRNA knockdown of ATF6 or XBP1 expression had no influence on G0S2 expression (Fig. 6D–E). Tunicamycin could also cause an appreciable elevation of G0S2 when ATF6 knockdown (Fig. 6I-K). As for IRE1α-XBP1 branch, IRE1α deficiency completely abolished tunicamycin-induced *Xbp1* expression but had no effect on *G0s2* and *Chop* in IRE1$^{-/-}$ MEF cells (Fig. 6F–H).

Knockdown of ATF4 in HepG2 cells resulted in significant reduction of *CHOP* (Supplementary Fig. 4A) as ATF4 directly binds to the composite site in *CHOP* promoter to induce its expression [18]. Interestingly, G0S2 level was significantly decreased in cells transfected with ATF4-siRNA (Fig. 6D–E), which could not be further enhanced by tunicamycin (Fig. 7B–C). To further verify whether the G0S2 transcription was ATF4 dependent, we conducted gain-of-function analysis in HepG2 cells with ATF4 plasmid. Overexpression of ATF4 in HepG2 cells greatly increased *G0S2* (Fig. 7E) and *CHOP* expression (Supplementary Fig. 4B). Taken together, these results demonstrated that ATF4 might be responsible for ER stress-driven G0S2 expression.

To illustrate whether G0S2 mediated ATF4-induced lipid accumulation, we exposed HepG2 cells to palmitate acid (PA) after co-expression of ATF4 with G0S2 siRNA. Oil-red O staining results revealed that lipid accumulation was increased in HepG2 cells with ATF4 overexpression, while G0S2 knockdown weakened the effect of ATF4 on lipid accumulation (Fig. 7I–H). These results clearly demonstrated the critical role of G0S2 in mediating the lipid metabolic effects of ATF4.

3.7. G0S2 was a direct ATF4 target gene

We further validated whether G0S2 is a direct transcriptional target of ATF4 with luciferase reporter assays. The *G0S2* promoter was activated under experimental ER stress conditions induced by tunicamycin (Fig. 8B). When ATF4 was co-expressed, the *G0S2* promoter luciferase activity was remarkably increased (Fig. 8C). Bioinformatics analysis identified a putative ATF4 binding core sequence in the promoter of *G0S2* genes of different species including mouse, rat and human. To identify whether the regulation of ATF4 on *G0S2* was dependent on the core sequence(CCGATA), a deletion mutant of *G0S2* promoter without the core sequence was constructed (Fig. 8D). The potentiating effect of ATF4 on *G0S2* promoter was lost in the deletion mutant (Fig. 8E). Finally, ChIP assay was performed to investigate whether ATF4 is bound to the *G0S2* promoter. Higher detectable amplification was observed in mice treated with tunicamycin compared to vehicle treated mice (Fig. 8F). Thus, *G0S2* could be formally classified as a direct ATF4 target gene.

4. Discussion

ER is notable for its central roles in lipid biosynthesis and the activation of UPR involves in obesity and obesity-related disorders [19]. In hepatocytes, ER stress is evident in several liver diseases, including obesity associated fatty liver disease [20], viral hepatitis [21] and alcohol-induced liver injury [22]. One of the key features of these liver disease is steatosis, raising the possibility that activation of ER stress contributes to development of metabolic syndrome [3]. Studies in animal models with genetic disruption of the IRE1α, ATF4, or ATF6 pathway indicates that all three UPR branches act in concert in regulating hepatic lipid homeostasis [23–25]. Treatment of obese and diabetic mice with chemical chaperones 4-PBA or TUDCA resulted in normalization of hyperglycemia, restoration of systemic insulin sensitivity, resolution of fatty liver disease [26]. Hence, abnormal lipid and glucose metabolism are important contributors to hepatic ER stress, and ER stress also plays an

Fig. 7. G0S2 is a direct transcriptional target of ATF4. HepG2 cells were transfected with ATF4 siRNA or control. After 48 h the transfected cells were then treated with DMSO or Tm (10 μg/ml) for 6 h ($n = 3$). (A, B) Quantitative real-time PCR was used to analyze *ATF4* and *G0S2* mRNA. (C) Expression of ATF4 and G0S2 protein were analyzed by immunoblotting in lysates from HepG2 cells transfected with ATF4 siRNA or control. HepG2 cells were transfected with ATF4 plasmid or control. After 24 h the transfected cells were then treated with treated with DMSO or Tm (10 μg/ml) for 6 h (n = 3). (D, E) Quantitative real-time PCR was used to analyze *ATF4* and *G0S2* mRNA. Results were shown as the mean ± SEM. *p < 0.05; ** p < 0.01; ***$p < 0.001$ by two-way ANOVA. (F) Expression of ATF4 and G0S2 protein were analyzed by immunoblotting in lysates from HepG2 cells transfected with ATF4 plasmid or control. (G) HepG2 cells were transfected with ATF4 plasmid and/or G0S2-siRNA. Expression of ATF4 and G0S2 protein were analyzed by immunoblotting in lysates from HepG2 cells. HepG2 cells were transfected with ATF4 plasmid and/or G0S2-siRNA. The transfected cells were treated with PA or BSA (control) for 12 h (n = 3). (I)Oil-red O staining was used to measure intracellular lipid accumulation in HepG2 cells. (H) The absorbance of Oil-red O dye at 520 nm. Results were shown as the mean ± SEM. * p < 0.05; ***p < 0.001 by one-way ANOVA.

important role in insulin resistance or fatty liver disease. Our study demonstrates that hepatic expression of the lipase inhibitor G0S2 is essentially dependent on hepatic ER stress. In our study, ER stress markers and G0S2 expression increased in all steatosis models. We observed an increase in G0S2 expression in tunicamycin-treated C57BL/6J mice and HepG2 cells where ER homeostasis was perturbed. Our findings suggest

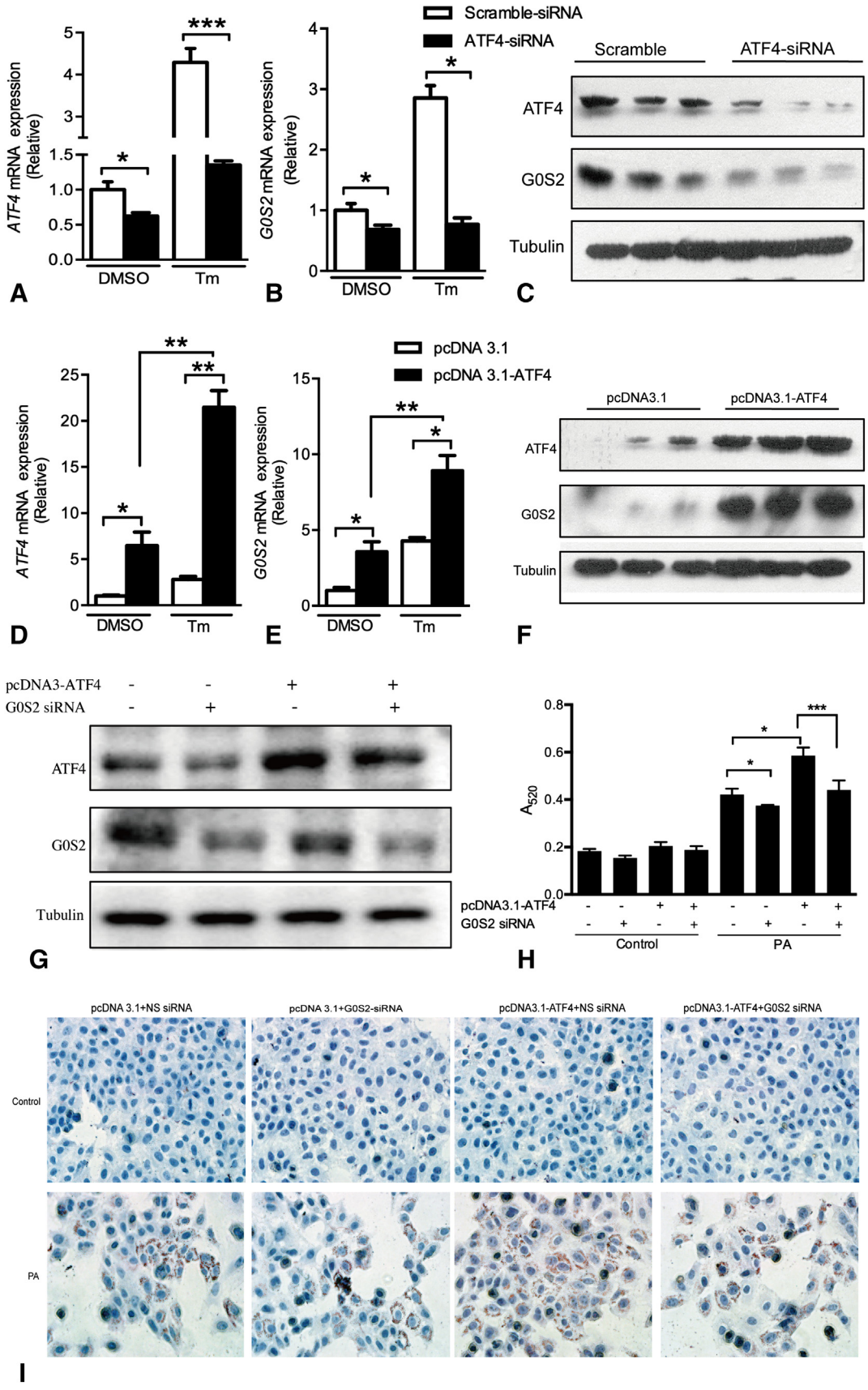

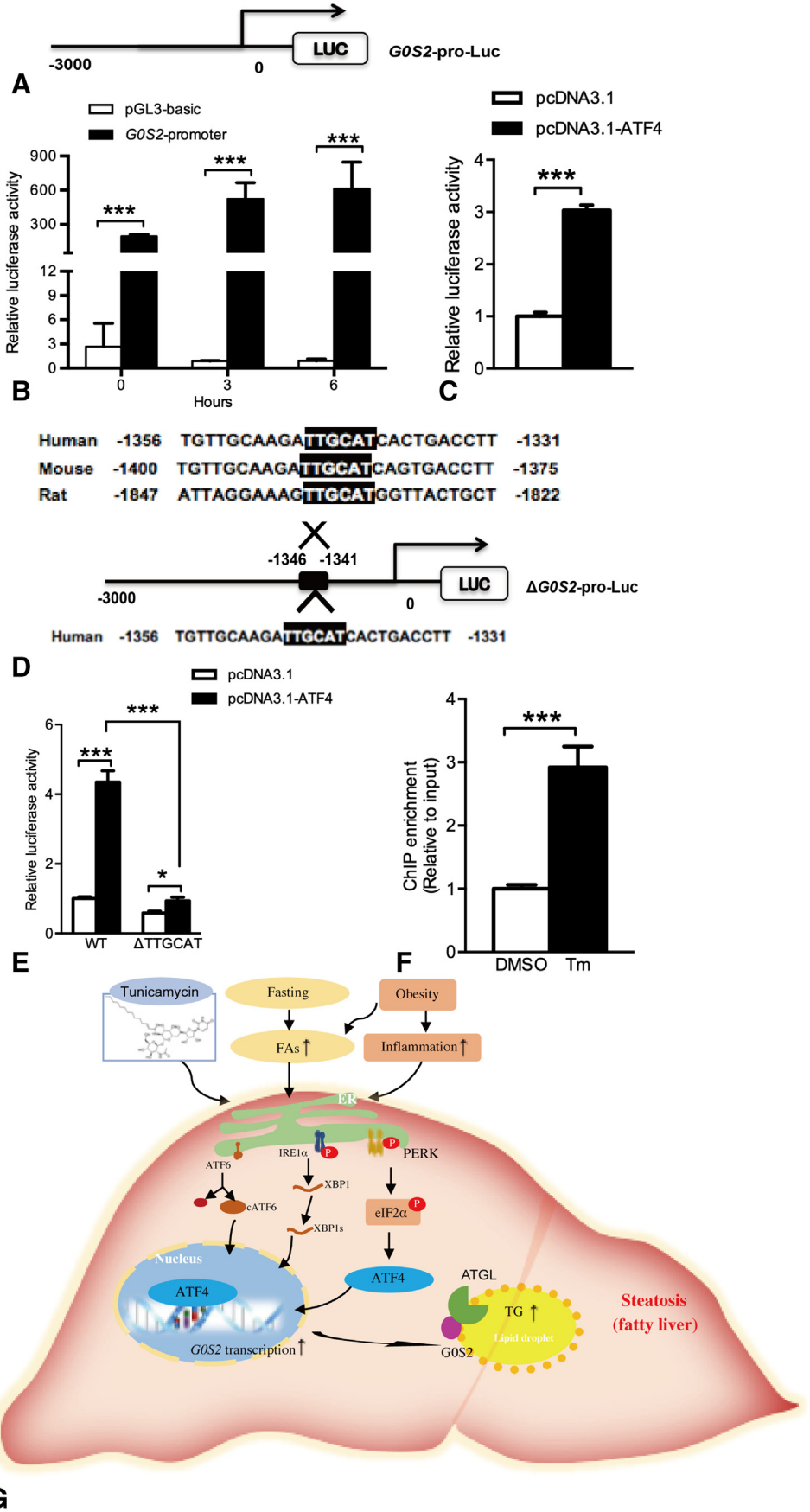
A
LUC
G0S2-pro-Luc
-3000
0
B
pGL3-basic
G0S2-promoter
Relative luciferase activity
Hours
C
pcDNA3.1
pcDNA3.1-ATF4
Relative luciferase activity
Human -1356 TGTTGCAAGATTGCATCACTGACCTT -1331
Mouse -1400 TGTTGCAAGATTGCATCAGTGACCTT -1375
Rat -1847 ATTAGGAAAGTTGCATGGTTACTGCT -1822
D
-1346 -1341
LUC
ΔG0S2-pro-Luc
-3000
0
Human -1356 TGTTGCAAGATTGCATCACTGACCTT -1331
E
pcDNA3.1
pcDNA3.1-ATF4
Relative luciferase activity
WT
ΔTTGCAT
F
ChIP enrichment (Relative to input)
DMSO
Tm
G
Tunicamycin
Fasting
Obesity
FAs
Inflammation
ER
IRE1α
PERK
ATF6
XBP1
cATF6
eIF2α
XBP1s
Nucleus
ATF4
ATF4
ATGL
TG
Lipid droplet
G0S2
G0S2 transcription
Steatosis
(fatty liver)

that changes in G0S2 expression might be reflecting the ER stress. To further validate whether G0S2 was the downstream target of ER stress, we employed chemical chaperones TUDCA to test if TUDCA could rescue elevated G0S2 expression during ER stress. As a result, suppression of ER stress significantly blunted tunicamycin-induced G0S2 expression. If G0S2 expression was directly linked to ER stress, which UPR pathway presumably contributed to the elevated G0S2 expression? Loss or gain function analysis found that PERK-eIF2α-ATF4 signaling pathway might specifically link to *G0S2* transcription. Furthermore, our evidence identified a core segment CCGATA in *G0S2* promoter, whose deletion diminished the occupancy of ATF4 on *G0S2* promoter.

Accumulated evidence suggests that ATF4, a basic leucine zipper transcription factor, plays a key role in controlling intracellular lipid accumulation by regulating genes involved in lipid metabolism, including both anabolism and catabolism [27]. For example, ATF4 increases intracellular lipid accumulation via activating expression such as sterol regulatory element-binding protein 1 (SREBP-1c), carbohydrate-responsive element-binding protein (ChREBP), FAS and SCD-1 [28,29] or being a negative regulator of PGC1α expression [30]. Similarly, our results revealed that *G0S2* was a new target gene of ATF4, which is most consistent with the phenotype that both ATF4-knockout mice and G0S2-knockout mice are protected from diet-induced hepatic steatosis [11,25].The above results indicate that G0S2 is a direct transcriptional target of ATF4. It is unknown whether G0S2 is linked to ER stress-induced progression of steatosis. Therefore, we examined the lipid droplet content in vitro by Oil-red O staining and found that suppression of G0S2 expression by G0S2 siRNA alleviated the effect of ATF4 on lipid accumulation. Collectively, these results suggested that ER stress-induced liver steatosis could be mediated, at least in part, via modulation of G0S2 expression in an ATF4 dependent fashion.

Metabolic disorders such as obesity, inflammation, insulin resistance, and type 2 diabetes have similar features with NAFLD, the hepatic component of metabolic syndrome. However it remains to be assessed whether ATF4-G0S2 axis is also involved in insulin resistance/hyperinsulinemia and type 2 diabetes. It was also found that G0S2 expression was significantly reduced in white adipose tissue of db/db mice and high-fat-fed wild-type mice [31]. They speculated that impaired insulin sensitivity of adipocytes may lead to the decreased expression of G0S2. However, when G0S2 level diminished, elevated basal lipolytic capacity of adipocytes is known to contribute to increased plasma FFA levels in human obesity [32]. The decreased G0S2 has the potential to increase lipolysis and circulating FFA concentrations as part of the pathogenesis of diabetic ketoacidosis and insulin resistance in metabolic syndrome and type 2 diabetes. Accordingly, further studies will be undertaken to investigate the relationship between the reduced level of G0S2 and insulin resistance associated with obesity.

Our results highlight the crucial role of ATF4-G0S2 axis in regulating hepatic TG deposition under ER stress. The identification of G0S2 as a direct transcriptional target of ATF4 links the PERK-eIF2α-ATF4 branch of the UPR to lipolysis, which provides a unique approach to treat NAFLD. However, our main findings of G0S2 expression and its lipid-regulating functions were obtained from studies in HepG2 cells. To further assess these results under physiologic conditions, more studies in vivo are needed to validate these observations. Hence, as a unique regulator of lipid metabolism, the intriguing role of G0S2 needs to be further explored. It is worth noting that ER stress is not the sole way regulating G0S2 expression. Upon fasting, enhanced exogenous FAs flow to the liver and hepatic TG levels sharply increase. LXRα-G0S2 axis has been found to be important in mediating fasting-induced hepatic TG accumulation [33]. Interestingly, recent reported studies also suggested that the increased abundance of hepatic G0S2 essentially depends on fatty acids when fasting [34]. Given that fasting-induced FAs can be sensed by hepatocyte ER thereby activating ER stress [5], ER stress-induced G0S2 expression may account for, at least partially, the increased level of hepatic TG accumulation when fasting. However, it has yet to be further investigated whether ATF4-G0S2 axis plays an essential role in hepatic TG accumulation during fasting. Moreover, given the role of ATF4 in hepatic lipid metabolism [35,36], it remains to be fully understood whether its downstream target G0S2 contributes mostly in ATF4-associated hepatosteatosis progression.

In summary, our evidence strongly demonstrated that G0S2 gene is a direct target gene of ATF4 pathway, which plays a crucial role in the progression of hepatic steatosis by inhibiting ATGL activity. Furthermore, we identified a conserved ATF4-binding sequence in the 5′ regulatory region of G0S2. Thus, modulation of ER stress or inhibition hepatic G0S2 expression may represent an effective way to enhance hepatic TG catabolism, thereby alleviating hepatic lipid accumulation and NAFLD progress.

Supplementary data to this article can be found online at https://doi.org/10.1016/j.metabol.2019.06.015.

Funding

This work was supported by the Natural Science Foundation of China (NSFC) NO. 81870598, NO. 81870616, NO. 11302130 and NSFC-NHMRC joint research grant NO. 81561128016, National Key Research and Development Program NO.2016YFC0903303, Municipal Natural Science Foundation of Shanghai NO. 17ZR1421200.

Author contributions

Weiping Jia and Haibing Chen designed the study and analyzed the results. Yunqin Ma and Mingliang Zhang performed the experiments, analyzed the results and wrote the paper. Hao Yong Yu, Junxi Lu, Jian Zhou and Kenneth KY Cheng reviewed the manuscript. All authors are guarantor of this work and take responsibility for the integrity of the data and the accuracy of the data analysis.

Acknowledgments

The authors thank the subjects who donated their surgical hepatic tissue samples to the study. We would also like to thank Dr. Jia LI of the Shanghai Institute of Materia Medica, Chinese Academy of Sciences for generously providing us with leptin-deficient mice. Thank Dr. Xu Shen from Shanghai Institute of Materia-Medica, Chinese Academy of Sciences who kindly provided us with pcDNA3.1-ATF4 plasmid.

Fig. 8. ATF4 trans-activates *G0S2* promoter by binding its conserved core site. (A) The luciferase reporter plasmid for the human *G0S2* promoter spanning the region from −3000 to 0 was constructed in pGL3-basic vector. (B) For luciferase activity assays, 293T cells were co-transfected with the *G0S2* promoter luciferase reporter plasmids (*G0S2*-pro-Luc) and renilla-expressing plasmid before treatment with Tm (10 μg/ml) for 3 h or 6 h. Results of luciferase activity were shown as the mean ± S.E.M and normalized to renilla-expressing plasmid fluorescence intensity. ***$p < 0.001$ by two-way ANOVA. (C) 293 T cells were co-transfected with the *G0S2*-pro-Luc, ATF4 plasmid and renilla-expressing plasmid plasmids for 36 h. Results of *G0S2* promoter luciferase activity were shown as the mean ± S.E.M and normalized to renilla-expressing plasmid fluorescence intensity. ***$p < 0.001$ by two-tailed Student *t*-test. (D) A potential ATF4 binding core site TTGCAT was identified which was conserved in the promoter of human, mouse and rat *G0S2* genes. (E) The deletion mutant luciferase reporter plasmid for the human *G0S2* promoter (−3000 to 0) that was short of the TTGCAT core sequence (Δ*G0S2*-pro-Luc) was constructed in pGL3-basic vector. 293T cells were co-transfected with *G0S2*-pro-Luc or Δ*G0S2*-pro-Luc, pcDNA3.1-ATF4 and renilla-expressing plasmid. Results of luciferase activity were shown as the mean ± S.E.M and normalized to renilla-expressing plasmid fluorescence intensity. *$p < 0.05$, ***$p < 0.001$ by two-way ANOVA. (F) Male C57BL/6J mice were treated with PBS (vehicle) or Tm (1 mg/kg body weight) ($n = 3$). ChIP assay of mouse liver nuclear extracts was carried out with control IgG or anti-ATF4 antibody. Results were shown as the mean ± S.E.M and input amplification was used for normalization. *** $p < 0.001$ by two-tailed Student *t*-test. (G) Schematic model. Excessive ER stress is associated with obesity-related metabolic dysregulation, adipose-derived FAs during fasting or ER stress inducer such as tunicamycin. PERK-eIF2α-ATF4 branch of the UPR plays a key role in the regulation of G0S2. As a directly target gene of ATF4, G0S2 alleviates ER stress-induced hepatic steatosis through inhibiting ATGL activity.

Declaration of Competing Interest

The authors declare no competing interests.

References

[1] Rector RS, Thyfault JP, Wei Y, Ibdah JA. Non-alcoholic fatty liver disease and the metabolic syndrome: an update. World J Gastroenterol 2008;14:185–92.
[2] Tamura S, Shimomura I. Contribution of adipose tissue and de novo lipogenesis to nonalcoholic fatty liver disease. J Clin Invest 2005;115:1139–42.
[3] Malhi H, Kaufman RJ. Endoplasmic reticulum stress in liver disease. J Hepatol 2011; 54:795–809.
[4] Ron D, Walter P. Signal integration in the endoplasmic reticulum unfolded protein response. Nat Rev Mol Cell Biol 2007;8:519–29.
[5] Fu S, Watkins SM, Hotamisligil GS. The role of endoplasmic reticulum in hepatic lipid homeostasis and stress signaling. Cell Metab 2012;15:623–34.
[6] Bobrovnikova-Marjon E, Hatzivassiliou G, Grigoriadou C, Romero M, Cavener DR, Thompson CB, et al. PERK-dependent regulation of lipogenesis during mouse mammary gland development and adipocyte differentiation. Proc Natl Acad Sci U S A 2008;105:16314–9.
[7] Lee AH, Scapa EF, Cohen DE, Glimcher LH. Regulation of hepatic lipogenesis by the transcription factor XBP1. Science 2008;320:1492–6.
[8] Zeng L, Lu M, Mori K, Luo S, Lee AS, Zhu Y, et al. ATF6 modulates SREBP2-mediated lipogenesis. EMBO J 2004;23:950–8.
[9] Schweiger M, Paar M, Eder C, Brandis J, Moser E, Gorkiewicz G, et al. G0/G1 switch gene-2 regulates human adipocyte lipolysis by affecting activity and localization of adipose triglyceride lipase. J Lipid Res 2012;53:2307–17.
[10] Russell L, Forsdyke DR. A human putative lymphocyte G0/G1 switch gene containing a Cpg-Rich Island encodes a small basic-protein with the potential to be phosphorylated. DNA Cell Biol 1991;10:581–91.
[11] Zhang X, Xie X, Heckmann BL, Saarinen AM, Czyzyk TA, Liu J. Targeted disruption of G0/G1 switch gene 2 enhances adipose lipolysis, alters hepatic energy balance, and alleviates high-fat diet-induced liver steatosis. Diabetes 2014;63:934–46.
[12] El-Assaad W, El-Kouhen K, Mohammad AH, Yang J, Morita M, Gamache I, et al. Deletion of the gene encoding G0/G 1 switch protein 2 (G0s2) alleviates high-fat-diet-induced weight gain and insulin resistance, and promotes browning of white adipose tissue in mice. Diabetologia 2015;58:149–57.
[13] Wang Y, Zhang Y, Qian H, Lu J, Zhang Z, Min X, et al. The g0/g1 switch gene 2 is an important regulator of hepatic triglyceride metabolism. PLoS One 2013;8: e72315.
[14] Nielsen TS, Moller N. Adipose triglyceride lipase and G0/G1 switch gene 2: approaching proof of concept. Diabetes 2014;63:847–9.
[15] Jiang S, Yan C, Fang QC, Shao ML, Zhang YL, Liu Y, et al. Fibroblast growth factor 21 is regulated by the IRE1alpha-XBP1 branch of the unfolded protein response and counteracts endoplasmic reticulum stress-induced hepatic steatosis. J Biol Chem 2014; 289:29751–65.
[16] Wong VW, Chan WK, Chitturi S, Chawla Y, Dan YY, Duseja A, et al. Asia-Pacific working party on non-alcoholic fatty liver disease guidelines 2017-part 1: definition, risk factors and assessment. J Gastroenterol Hepatol 2018;33:70–85.
[17] Kleiner DE, Brunt EM, Van Natta M, Behling C, Contos MJ, Cummings OW, et al. Design and validation of a histological scoring system for nonalcoholic fatty liver disease. Hepatology 2005;41:1313–21.
[18] Ma Y, Brewer JW, Diehl JA, Hendershot LM. Two distinct stress signaling pathways converge upon the CHOP promoter during the mammalian unfolded protein response. J Mol Biol 2002;318:1351–65.
[19] Pagliassotti MJ, Kim PY, Estrada AL, Stewart CM, Gentile CL. Endoplasmic reticulum stress in obesity and obesity-related disorders: an expanded view. Metabolism 2016;65:1238–46.
[20] Ozcan U, Cao Q, Yilmaz E, Lee AH, Iwakoshi NN, Ozdelen E, et al. Endoplasmic reticulum stress links obesity, insulin action, and type 2 diabetes. Science 2004;306: 457–61.
[21] Chan SW. Unfolded protein response in hepatitis C virus infection. Front Microbiol 2014;5:233.
[22] Longato L, Ripp K, Setshedi M, Dostalek M, Akhlaghi F, Branda M, et al. Insulin resistance, ceramide accumulation, and endoplasmic reticulum stress in human chronic alcohol-related liver disease. Oxid Med Cell Longev 2012;2012:479348.
[23] Zhang K, Wang S, Malhotra J, Hassler JR, Back SH, Wang G, et al. The unfolded protein response transducer IRE1alpha prevents ER stress-induced hepatic steatosis. EMBO J 2011;30:1357–75.
[24] Chen X, Zhang F, Gong Q, Cui A, Zhuo S, Hu Z, et al. Hepatic ATF6 increases fatty acid oxidation to attenuate hepatic steatosis in mice through peroxisome proliferator-activated receptor alpha. Diabetes 2016;65:1904–15.
[25] Li K, Xiao Y, Yu J, Xia T, Liu B, Guo Y, et al. Liver-specific gene inactivation of the transcription factor ATF4 alleviates alcoholic liver steatosis in mice. J Biol Chem 2016; 291:18536–46.
[26] Ozcan U, Yilmaz E, Ozcan L, Furuhashi M, Vaillancourt E, Smith RO, et al. Chemical chaperones reduce ER stress and restore glucose homeostasis in a mouse model of type 2 diabetes. Science 2006;313:1137–40.
[27] Wang C, Guo F. Effects of activating transcription factor 4 deficiency on carbohydrate and lipid metabolism in mammals. IUBMB Life 2012;64:226–30.
[28] Li H, Meng Q, Xiao F, Chen S, Du Y, Yu J, et al. ATF4 deficiency protects mice from high-carbohydrate-diet-induced liver steatosis. Biochem J 2011;438:283–9.
[29] Ren LP, Yu X, Song GY, Zhang P, Sun LN, Chen SC, et al. Impact of activating transcription factor 4 signaling on lipogenesis in HepG2 cells. Mol Med Rep 2016;14: 1649–58.
[30] Wang C, Xia T, Du Y, Meng Q, Li H, Liu B, et al. Effects of ATF4 on PGC1alpha expression in brown adipose tissue and metabolic responses to cold stress. Metabolism 2013;62:282–9.
[31] Yang X, Lu X, Lombes M, Rha GB, Chi YI, Guerin TM, et al. The G(0)/G(1) switch gene 2 regulates adipose lipolysis through association with adipose triglyceride lipase. Cell Metab 2010;11:194–205.
[32] Guilherme A, Virbasius JV, Puri V, Czech MP. Adipocyte dysfunctions linking obesity to insulin resistance and type 2 diabetes. Nat Rev Mol Cell Biol 2008;9: 367–77.
[33] Heckmann BL, Zhang X, Saarinen AM, Schoiswohl G, Kershaw EE, Zechner R, et al. Liver X receptor alpha mediates hepatic triglyceride accumulation through upregulation of G0/G1 switch gene 2 expression. JCI Insight 2017;2:e88735.
[34] Jaeger D, Schoiswohl G, Hofer P, Schreiber R, Schweiger M, Eichmann TO, et al. Fasting-induced G0/G1 switch gene 2 and FGF21 expression in the liver are under regulation of adipose tissue derived fatty acids. J Hepatol 2015;63:437–45.
[35] Seo J, Fortuno 3rd ES, Suh JM, Stenesen D, Tang W, Parks EJ, et al. Atf4 regulates obesity, glucose homeostasis, and energy expenditure. Diabetes 2009;58: 2565–73.
[36] Wang C, Huang Z, Du Y, Cheng Y, Chen S, Guo F. ATF4 regulates lipid metabolism and thermogenesis. Cell Res 2010;20:174–84.